Entry of a heparan sulphate-binding HRV8 variant strictly depends on dynamin but not on clathrin, caveolin, and flotillin

Abdul Ghafoor Khan [a],[1], Angela Pickl-Herk [a], Leszek Gajdzik [b], Thomas C. Marlovits [c], Renate Fuchs [b], Dieter Blaas [a],*

[a] *Dept. Med. Biochem., Max F. Perutz Laboratories, Vienna Biocenter, Medical University of Vienna, Dr. Bohr Gasse 9/3, A-1030 Vienna, Austria*
[b] *Department of Pathophysiology, Medical University of Vienna, Vienna, Austria*
[c] *IMP — Institute of Molecular Pathology and IMBA — Institute of Molecular Biotechnology GmbH, Vienna, Austria*

ARTICLE INFO

ABSTRACT

The major group human rhinovirus type 8 can enter cells via heparan sulphate. When internalized into ICAM-1 negative rhabdomyosarcoma (RD) cells, HRV8 accumulated in the cells but caused CPE only after 3 days when used at high MOI. Adaptation by three blind passages alternating between RD and HeLa cells resulted in variant HRV8v with decreased stability at acidic pH allowing for productive infection in the absence of ICAM-1. HRV8v produced CPE at 10 times lower MOI within 1 day. Confocal fluorescence microscopy colocalization and the use of pharmacological and dominant negative inhibitors revealed that viral uptake is clathrin, caveolin, and flotillin independent. However, it is blocked by dynasore, amiloride, and EIPA. Furthermore, HRV8v induced FITC-dextran uptake and colocalized with this fluid phase marker. Except for the complete inhibition by dynasore, the entry pathway of HRV8v via HS is similar to that of HRV14 in RD cells that overexpress ICAM-1.

© 2010 Elsevier Inc. All rights reserved.

Introduction

Human rhinoviruses are a major cause of the common cold (Heikkinen and Jarvinen, 2003). They include three species (HRV-A, B, and C) of the genus Enterovirus, family *Picornaviridae* (Palmenberg et al., 2009). Twelve HRV-A (the minor receptor group) (Vlasak et al., 2005b), bind low-density lipoprotein receptor (LDLR), LDLR related protein (LRP) (Hofer et al., 1994), and very-LDLR (VLDLR) (Marlovits et al., 1998), while the remaining 61 HRV-A and all 26 HRV-B utilize intercellular adhesion molecule 1 (ICAM-1) for cell entry and infection (Uncapher et al., 1991). The receptor(s) of the recently discovered HRV-C clade is not known (McErlean et al., 2008). The minor group virus HRV2 is internalized via the well-characterized clathrin-dependent endocytic pathway (Snyers et al., 2003); however, similar to other ligands, it can switch to different entry portals when this pathway is blocked (Bayer et al., 2001). Having once arrived in endosomal carrier vesicles or late endosomes, uncoating is triggered

by the acidic pH (Konecsni et al., 2009; Neubauer et al., 1987; Prchla et al., 1994). Conversely, in major group HRVs the process is initiated by the receptor, ICAM-1, itself (Bayer et al., 1999; Greve et al., 1991) but assisted by the low endosomal pH (Nurani et al., 2003).

Attempts at adapting the major group HRV89 to bind LDL-receptors resulted in variants replicating in cells lacking ICAM-1 expression (Reischl et al., 2001; Vlasak et al., 2005a). HRV54 was even able to multiply in ICAM-1 negative rhabdomyosarcoma (RD) cells without prior adaptation. However, HRV54 wt as well as the above HRV89 variants had not acquired affinity for LDL-receptors but rather bound heparan sulphate (HS) and preserved their ability to attach to ICAM-1 (Khan et al., 2007).

HS is present ubiquitously on the surface of most animal cells and in the extracellular matrix where it has been implicated in numerous biological functions including cell–matrix and cell–cell adhesion, cell proliferation, motility and differentiation, blood coagulation, inflammation, tumor progression and invasion, tissue regeneration, lipoprotein metabolism and pathogen infections (reviewed in Bishop et al., 2007). Although many ligands and viruses attach to HS proteoglycans, data on cellular uptake are controversial. For example, entry of cationic peptides binding to HS was ascribed either to the clathrin-, the caveolin-, or the macropinocytic machinery (Duchardt et al., 2007; Jones, 2007; Poon and Gariepy, 2007). Eosinophil cationic

---

* Corresponding author. Fax: +43 1 4277 9616.
  E-mail address: dieter.blaas@meduniwien.ac.at (D. Blaas).
[1] Present address: NUST Center of Virology and Immunology (NCVI), National University of Sciences and Technology (NUST), sector H-12, Islamabad, Pakistan.

protein, when attaching to HS on human bronchial epithelial Beas-2B cells exhibited characteristics of raft-dependent macropinocytosis (Fan et al., 2007). Finally, HS-binding cationic polyplexes and antibodies against HS were shown to enter in the absence of functional clathrin and caveolin but co-localized with flotillin and trafficked to late endosomes (Payne et al., 2007). An increasing number of viruses have also been shown to use HS as (an alternative) receptor but again, their entry pathway into the host cell is largely ignored (Spillmann, 2001). These ambiguous results indicate that uptake via HS is poorly understood. The involvement of proteoglycans in viral infection and drug delivery underscores the importance to investigate the mechanism underlying their uptake. We here report on entry and trafficking of HRV8v, a variant that binds HS and was selected for replication in ICAM-1 negative rhabdomyosarcoma (RD) cells. Employing pharmacological compounds, specific dominant-negative inhibitors, and immunofluorescence colocalization microscopy, we demonstrate that HRV8v enters RD cells via a dynamin-dependent pathway that is independent of clathrin, caveolin, and flotillin.

Results

Wild type HRV8 enters rhabdomyosarcoma cells but replicates inefficiently

HRV8 wt gave rise to CPE in ICAM-1 negative RD cells only upon challenge at >100 TCID50/cell after three days. However, upon continuous internalization for 30 min it readily entered RD cells and accumulated in vesicular structures seen by confocal immunofluorescence microscopy of a single confocal slice through the cell body (Fig. 1A and movie of deconvolved image stacks in Supplementary material). Previously, we obtained variants of HRV89 (HRV89M) upon 34 serial blind passages alternating between HeLa and Hep-2 cells that were able to replicate in these latter (ICAM-1 negative) cells (Reischl et al., 2001; Vlasak et al., 2005a). For HRV8, only three such passages in HeLa and RD cells were required for the appearance of a variant (HRV8v) that replicated and produced CPE equally in RD cells stably transfected to express human ICAM-1 (Newcombe et al., 2003) and in RD wild type cells. HRV8v was less stable at low pH than wt HRV8; at pH 5.6, a reduction of infectivity by almost 3 logs was observed (Fig. 1B). This pH value is attained in endosomal carrier vesicles and late endosomes in HeLa cells where it triggers uncoating of the minor group virus HRV2 (Brabec et al., 2003; Gruenberger et al., 1991). In the absence of the 'catalytic' activity of ICAM-1, HRV8v must be uncoated by the low pH. Thus, decreased viral stability in acidic environment correlates with productive infection in the ICAM-1 negative RD cells.

Employing the same strategy previously used to identify heparan sulphate (HS) proteoglycan as an alternative receptor for HRV54 (Khan et al., 2007) and the HRV89 variants mentioned above, it became clear that HRV8 also attaches to HS. This is exemplified by the inhibition of binding to RD cells with heparin (Fig. 2A), significantly reduced binding to CHO mutant cell lines pgsA-745 and pgsD-677 (Fig. 2B), and the complete inhibition of infection of RD cells by HRV8v in the presence of heparin (Fig. 2C). PgsA-745 is deficient in xylosyltransferase synthesis and unable to produce glycosaminoglycans whereas pgsD-677 is doubly deficient in N-acetylglucosaminyltransferase and glucuronyltransferase and fails to synthesize HS but produces threefold-higher levels of chondroitin sulphate than wt. As for the minor group virus HRV2 (Bayer et al., 1998) and the HS-adapted variants above, HRV8v infection via HS was completely blocked by bafilomycin A1, an inhibitor of endosomal H$^+$-ATPases. On the other hand, in RD-ICAM cells development of CPE was only slightly affected by the drug (not shown). Collectively, these data demonstrate that the more stable wt virus, although entering RD cells, only inefficiently uncoats without the aid of ICAM-1. Therefore, apart from receptor selection and entry, uncoating is a major determinant
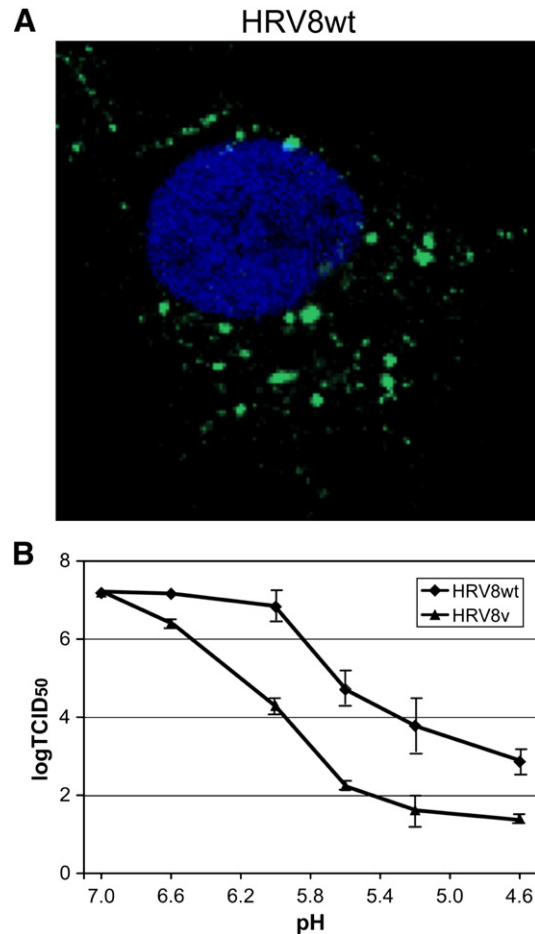

Fig. 1. HRV8 wt uncoating but not entry correlates with poor infection of ICAM-1 negative RD cells. A) RD cells were grown on glass cover slips and infected with HRV8 wt at 300 TCID$_{50}$/cell at 34 °C. After 30 min of continuous internalization, cells were washed and fixed with 4% paraformaldehyde. HRV8 was revealed with mouse antiserum followed by Alexa Fluor 488 secondary antibody. Nuclei were stained with DAPI. Cells were viewed under a LSM510 confocal microscope; one focal plane through the cell body is shown. B) Virus at 10^7 TCID$_{50}$ was incubated at 34 °C for 30 min in isotonic 100 mM MES buffer of the indicated pH values and, after re-neutralization, infectivity was determined by endpoint dilution. Mean and SD of 4 independent experiments.

for efficient infection. Note that all subsequent experiments were carried out with HRV8v to allow for functional assays (i.e. readout of entry/uncoating via cleavage of eIF4G and viral replication).

HRV8v shows different staining patterns when entering via ICAM-1 or via HS

HRV2 enters via clathrin-mediated endocytosis (CME) and HRV14 via a non-clathrin, non-caveolin, non-flotillin dependent route (Khan et al., 2010; Snyers et al., 2003). To study whether HRV8v follows any of these pathways, RD cells were co-infected with HRV8v and HRV2 for 30 min followed by fixation, specific staining, and immunofluorescence confocal microscopy. As seen in Fig. 3 (upper panels), there is only a marginal overlap (arrowheads) indicating that the two virus types localize to distinct compartments. HRV2 is delivered into early (EEA1-positive) endosomes and then transferred into late endosomes. Some of the HRV8v appears to attain also this early compartment. When the same experiment was conducted with HRV89M, another HS-binding variant (see above and Vlasak et al., 2005a), essentially complete overlap was observed (Fig. 3, middle panel). Co-localization was also evident upon internalization of HRV8v together with HRV14 in RD-ICAM cells, although the pattern
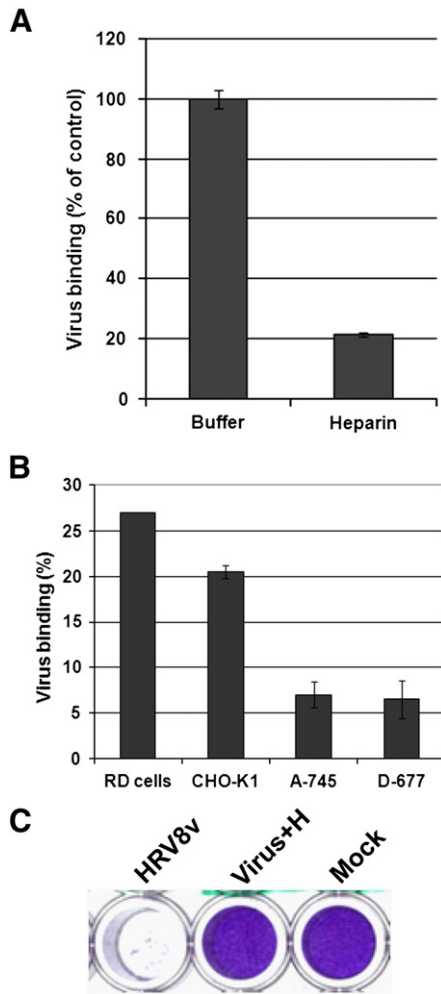
Fig. 2. In RD cells HRV8 binding and HRV8v infection depend on heparan sulphate. A) RD cells grown in 24-well plates until almost confluent were incubated with about 12,000 cpm of [^{35}S]-labeled HRV8 for 1 h at room temperature in the absence or the presence of 2 mg/ml heparin. Cells were washed with PBS and trypsinized and cell associated radioactivity was determined by liquid scintillation counting. B) RD cells, CHO-K1 (wild type control), and the mutants pgsA-745 and pgsD-677 grown in 6 well plates were incubated with [^{35}S]-labeled HRV8 as above, trypsinized, and scintillation counted as above. Cell-associated radioactivity is given as percentage of total radioactivity. Mean +/- SD of three experiments. C) RD cells grown in 96-well plates were challenged with HRV8v at 10 TCID$_{50}$/cell in the absence and in the presence of 2 mg/ml heparin and stained with crystal violet at 24 h pi.

very much differed from that produced in RD cells (compare lower panels with upper panels). Presumably, this relates to the high expression level of ICAM-1, which results in binding of large amounts of virus and predominant uptake via this receptor. Taken together, the above observations demonstrate that entry and intracellular trafficking of HRV2 and HRV8v are distinct. Unfortunately, because of its dual receptor specificity, with this type of experiment it is not possible to find out whether HRV8v (when exclusively entering via HS) and HRV14 (entering via ICAM-1) exploit different pathways.

Virus entry via HS is clathrin-independent

Because of the different intracellular localization of HRV2 and HRV8v during continuous internalization, clathrin-dependent entry for the latter virus is unlikely. For confirmation, HRV8v was co-internalized with human transferrin, a marker for CME. Cells were washed and fixed after 5 and 15 min of continuous co-internalization. Note that attachment of HRV8v was found to be slow, particularly at low temperature. This precluded examination of virus localization at

times shorter than 5 min. It is well known and also demonstrated by our laboratories that under these conditions, most of the Alexa Fluor 568-labeled transferrin localizes in early endosomes and in the perinuclear region at 5 min (Baravalle et al., 2005); confocal immunofluorescence microscopy demonstrated a clear separation from HRV8v that largely remained at the cell periphery (Fig. 4A). At 15 min, transferrin had accumulated in the perinuclear region whereas HRV8v was evenly distributed throughout the cell body. Notably, co-localization, as determined with BioImageXD was about 1% at both time points. HRV2, used as a control, completely overlapped with transferrin (90% overlap; not shown), although their intracellular pathways separate rapidly (Brabec et al., 2006). These data demonstrate that transferrin and HRV8v enter with different kinetics and localize to different compartments, making CME for HRV8v entry via HS improbable.

Direct proof for clathrin-independent entry via HS was obtained by using a GFP-tagged clathrin light chain. RD cells overexpressing GFP-clathrin were challenged with virus and fixed at 5 and 15 min pi. In accordance with the previous results, there was no colocalization between GFP-clathrin and HRV8v at either time (Fig. 4B) whereas transferrin used as a control overlapped with GFP-clathrin at the early time point (not shown).

Dominant negative inhibitors of clathrin-mediated endocytosis do not affect virus entry

For further confirmation of clathrin-independence, we used dominant-negative (DN) mutants that potently interfere with the normal functions of key proteins of the clathrin-dependent pathway. The SH3 domain of amphiphysin (amphi-SH3) has been shown to inhibit receptor mediated endocytosis of HRV2, transferrin, and epidermal growth factor (Snyers et al., 2003; Wigge et al., 1997) by impeding recruitment of dynamin to coated pits. Accordingly, RD cells were transfected with myc-tagged amphi-SH3 followed by infection with HRV8v. Confocal microscopy revealed no difference in entry in the presence or absence of amphi-SH3 expression (Fig. 5, upper panels). To assess clathrin function more directly, we also used the C-terminal domain of AP180 (AP180-C), which has been shown unequivocally to inhibit CME (Ford et al., 2001). Overexpression of DN AP180-C also failed to modify entry of HRV8v in RD cells (Fig. 5, lower panels); in contrast, both DN inhibitors readily prevented transferrin internalization (Fig. 5, right panels). No staining of viral protein was seen in the absence of permeabilization (not shown).

HRV8v colocalizes neither with cholera toxin B nor with caveolin-1

The caveolin pathway is the second best characterized cell entry route. Although for various HS-binding ligands a macropinocytic entry mode has been suggested, entry of FMDV via HS was reported to be impaired upon knocking down caveolin-1 in MCF-10A cells (O'Donnell et al., 2008). Thus, it was of interest to investigate carefully the involvement of caveolin in HRV8v virus entry. A possible role of caveolin was evaluated by assessing co-localization of virus with cholera toxin subunit B (CtxB). CtxB is a widely accepted marker of this pathway although it has also been shown in association with flotillin- (Glebov et al., 2006) and clathrin-dependent endocytosis in various cell types (Hansen et al., 2005; Torgersen et al., 2001). RD cells were challenged with HRV8v in the presence of Alexa Fluor 488 CtxB for 5 and 15 min at 34 °C, washed, and fixed. Confocal microscopy showed both ligands close to the cell surface but in distinct locations at 5 min. At 15 min, CtxB had moved to the Golgi and concentrated in the perinuclear region while HRV8v remained spread throughout the cytosol (Fig. 6A). Again, there was virtually no colocalization (1% at 5 min and 5% at 15 min as determined with BioImageXD). These results indicate that HRV8v and CtxB use different pathways to different destinations within the cell. CtxB accumulated in typical
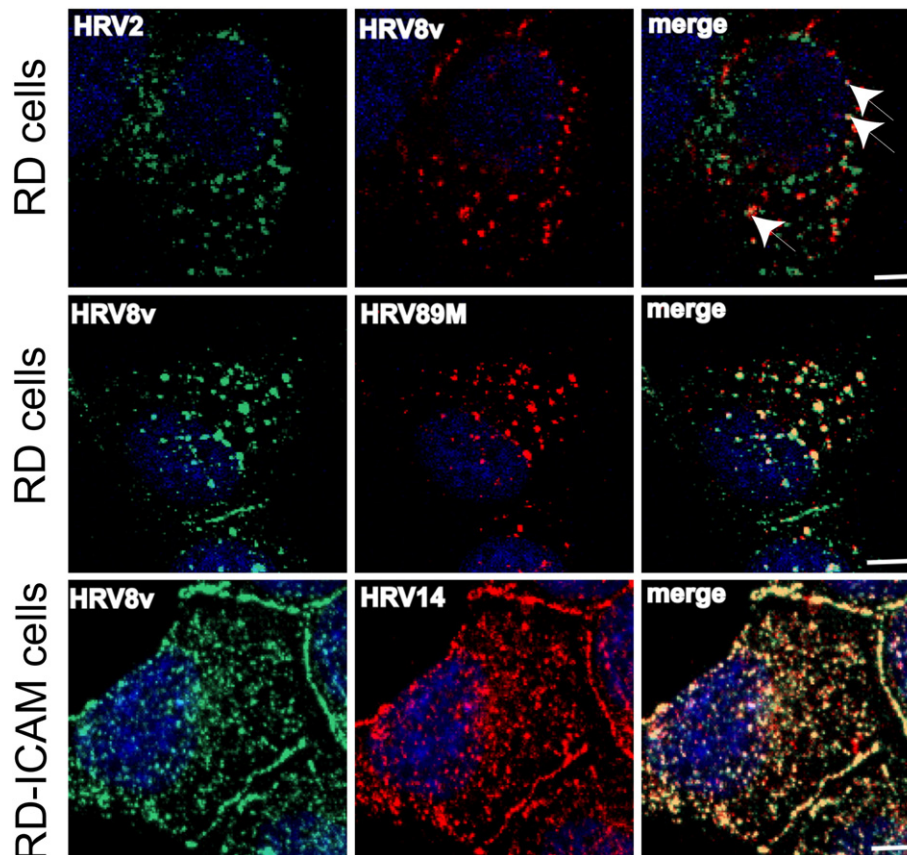
Fig. 3. HRV8v entering via HS or via ICAM-1 exhibits distinct intracellular localization patterns. RD cells (upper two rows) were challenged with pairs of the virus types indicated at 300 $TCID_{50}$/cell for 30 min at 34 °C. Cells were washed and fixed, and the respective virus was stained with corresponding type-specific antibody, followed by TxR- and Alexa Fluor 488-labeled secondary antibodies and viewed under a confocal microscope. Lower row, RD-ICAM cells were used. HRV89M is a HS-binding variant (Vlasak et al., 2005a). Nuclei were stained with DAPI. Arrowheads point to sites of colocalization. Ten confocal stacks were combined. Bar, 10 μm.

Golgi structures at 30 min. However, even after 1 h HRV8v failed to colocalize with CtxB (data not shown). These results definitely exclude HRV8v transport to the Golgi. Further confirmation by more direct means was obtained via transfecting cells with caveolin-1 tagged with GFP, either at the N- (GFP-caveolin) or the C-terminus (caveolin-GFP). The former construct also acts as a DN inhibitor of caveolin function (Pelkmans et al., 2001). HRV8v colocalized neither with GFP-caveolin nor with caveolin-GFP (Fig. 6B), furthermore, expression of GFP-caveolin did not inhibit viral entry. We also stained caveolin-1 by using anti-caveolin antibodies and assessed eventual colocalization. Consistent with the previous results, no colocalization of virus and caveolin-1 was observed (data not shown). We also noticed that RD cells express very low levels of caveolin-1 while HeLa and CHO cells contain high amounts of this protein. Nevertheless, virus entry and eIF4G cleavage (see below) occurred equally in RD and CHO-K1 cells (not shown). These results clearly exclude the involvement of caveolin-1 in entry and intracellular trafficking of HRV8v via HS in RD cells.

Entry via HS is flotillin-1 independent

Flotilin-1 and -2 have been described as markers of a clathrin and caveolin-independent pathway (Glebov et al., 2006) and more recent data suggested involvement of flotillin-1 in uptake of HS-binding ligands (Payne et al., 2007). Therefore, having excluded entry of HRV8v via clathrin- and caveolin-dependent routes it was of interest to investigate whether flotillin-1 was involved. Again, by using immunofluorescence microscopy, colocalization with flotillin-1 was assessed. As shown in Fig. 7, flotillin-1 staining did not overlap with

HRV8v (1% colocalization at both time points). Therefore, it is unlikely that flotillin-1 takes part in entry of HRV8v into RD cells via HS.

HRV8v induces fluid-phase uptake and colocalizes with FITC-dextran

Next, we studied macropinocytosis as a candidate pathway for viral entry. RD cells were challenged with HRV8v in the presence of 500 μg/ml of the fluid-phase marker FITC-dextran for 15 and 30 min at 34 °C. Cells were fixed and examined by confocal fluorescence microscopy. Fig. 8A shows substantial (38%) colocalization of HRV8v with FITC-dextran, which is considered 'a relatively specific marker of macropinocytosis' (Falcone et al., 2006). These results suggest that uptake via HS might occur by macropinocytosis. In the majority of cell types macropinocytosis is not a constitutive process but is induced by growth factors or viruses (Mercer and Helenius, 2009). As seen in Fig. 8B, uptake of FITC-dextran was stimulated upon challenge of RD cells with HRV8v. This stimulation was even stronger than that of epidermal growth factor (EGF) used as a control. In accordance with data on macropinocytosis of adenovirus (Meier et al., 2002), dextran uptake decreased again at 30 min (not shown).

Pharmacologic inhibitors point to HRV8v entry via macropinocytosis

Finally, we examined the effect of various drugs on viral entry and replication. These substances have been extensively employed to specifically inhibit particular endocytic pathways. As in previous work on HRV14 entry (Khan et al., 2010), we made use of cleavage of the translation initiation factor eIF4GI as readout. This allows cutting down the time of exposure to the drugs and thereby to minimize side effects. Upon uncoating, the viral RNA is released into the cytoplasm
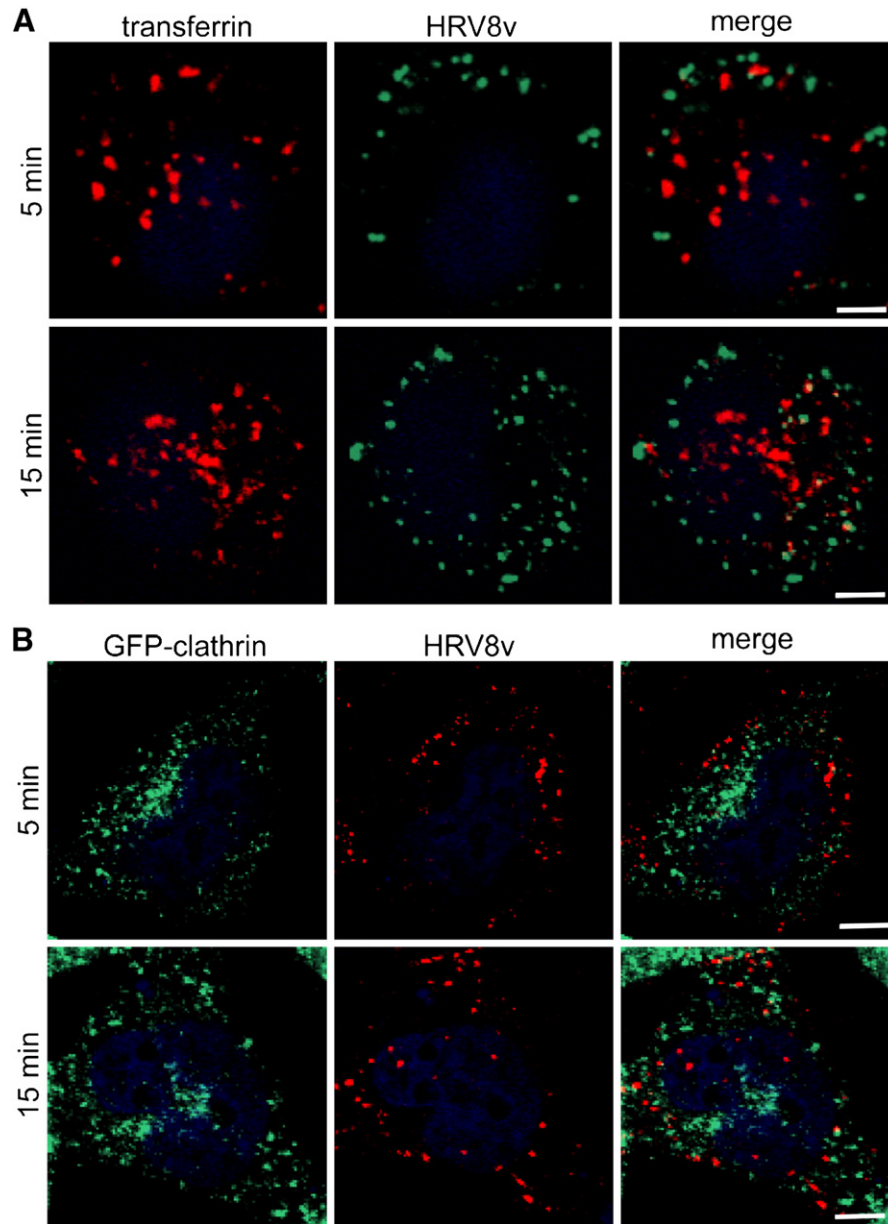
Fig. 4. HRV8v neither colocalizes with transferrin nor with GFP-clathrin. A) RD cells were incubated with HRV8v at 500 $TCID_{50}$/cell along with 10 μg/ml Alexa Fluor 568-transferrin for 5 and 15 min at 37 °C (continuous internalization). Unbound material was washed away, and cells were fixed and stained for virus with type-specific mouse antiserum followed by Alexa Fluor 488-labeled secondary antibody. B) RD cells were transfected with pEGFP-clathrin light chain and after 24 h cells were infected with HRV8v and processed as above. Colocalization was assessed by confocal fluorescence microscopy. One confocal slice is shown. Bar, 10 μm.

and is translated into a polyprotein; autocatalytic cleavage sets free the viral proteinase 2A that efficiently cleaves eIF4GI into fragments that can be easily detected at 3 h pi. Thus, cleavage of eIF4GI is suitable as a functional assay for productive entry as it only takes place on arrival of the viral RNA in the cytosol and does not require viral replication (Gradi et al., 1998). RD cells were pre-incubated with the drugs indicated in Fig. 9A for 30 min, challenged with HRV8v, and collected after 3 h. As previously described for poliovirus (Irurzun and Carrasco, 2001) and HRV14 (Khan et al., 2010), cleavage of eIF4GI was assessed via western blot analysis. Unprocessed eIF4GI and its proteolysis products were quantified with ImageJ by using scanned X-ray films (Fig. 9B).

Although chlorpromazine (CPZ) is known to possess a number of pleiotropic and cell type specific effects, it has been extensively used to demonstrate CME of viruses (see for example Akula et al., 2003; Pu and Zhang, 2008; Raghu et al., 2009; Van Hamme et al., 2008). In agreement with the results above, eIF4GI cleavage upon HRV8v infection was not inhibited by CPZ. Conversely, chlorpromazine completely blocked eIF4GI cleavage in cells incubated with HRV2 that was used as a control (Khan et al., 2010 and data not shown).

Caveolin-mediated endocytosis is associated with lipid rafts. Removal or sequestering of cholesterol profoundly inhibits entry of CtxB and other ligands internalized via this route (Schnitzer et al., 1994). Nystatin destroys the rafts by intercalating between cholesterol molecules while methyl-ß-cyclodextrin (MßCD) extracts the cholesterol from the membranes. Both result in impairment of caveolin/lipid raft-dependent endocytosis. Whereas MßCD might also affect CME and raft-dependent macropinocytosis, nystatin acts more specifically on caveolar endocytosis (Smart and Anderson, 2002; Stuart et al., 2002). MßCD decreased eIF4GI cleavage caused by HRV8v infection by about 50% whereas nystatin was essentially without effect. Together with the results above, this makes it unlikely that caveolin is involved but suggests that lipid rafts may play some minor role in HRV8v entry.
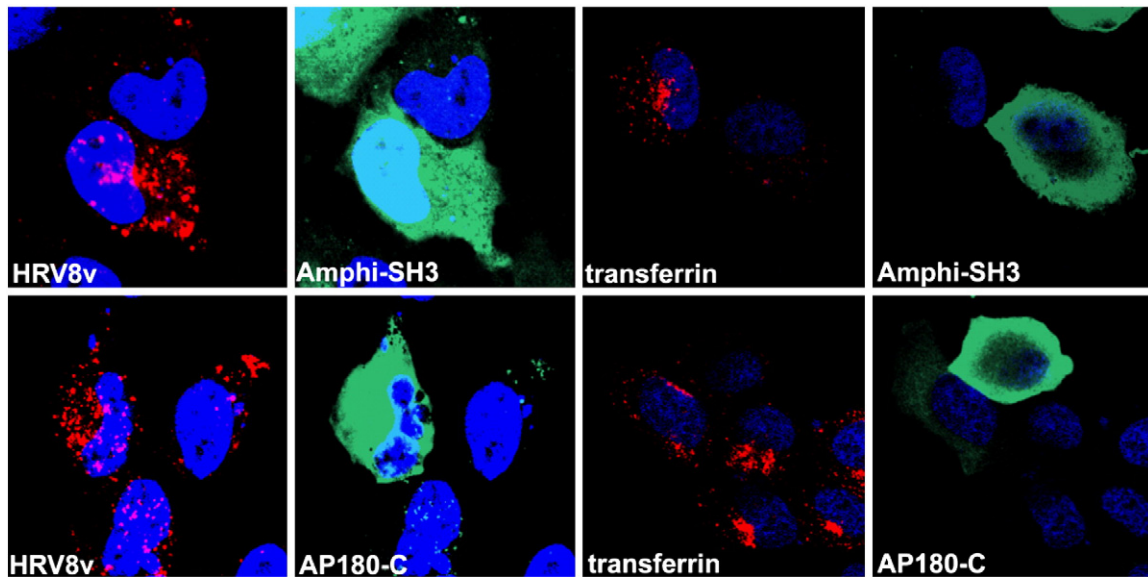
Fig. 5. Dominant negative inhibitors of the clathrin-dependent pathway do not affect HRV8v entry. RD cells were transfected with DN myc-tagged amphi-SH3 and AP180-C as indicated and challenged with HRV8v at 300 TCID$_{50}$/cell for 30 min at 34 °C (continuous internalization). Virus was detected with type-specific antiserum and TxR-labeled secondary antibody, whereas expression of the DN inhibitors was assessed by using mouse anti-myc mAb followed by Alexa Fluor 488-labeled secondary antibody. Transferrin Alexa Fluor 568 was used as a control. Samples were processed and viewed as in Fig. 2. One confocal slice is shown. Bar, 10 μm.

Amiloride and its derivative 5-(N-ethyl-N-isopropyl) amiloride (EIPA) inhibit the Na+/H+ exchangers (Masereel et al., 2003). Employed at mM and higher μM concentrations, respectively, they have been demonstrated to inhibit macropinocytosis of various viruses and other ligands (Kalin et al., 2010; Karjalainen et al., 2008; Schneider et al., 2007; West et al., 1989). The underlying mechanism has been revealed only very recently (Koivusalo et al., 2010); they appear to arrest cargo in a compartment close to the plasma membrane and inaccessible from outside (Liberali et al., 2008). Cytochalasin D, on the other hand, inhibits membrane ruffling and re-organization of the actin cytoskeleton that are required for plasma membrane engulfment of liquid and ligands. Amiloride/EIPA completely inhibited cleavage of eIF4GI by HRV8v while cytochalasin inhibited strongly, although not completely. Dynasore, an inhibitor of the GTPase dynamin (Macia et al., 2006) that is involved in membrane fission in a number of endocytic pathways (Doherty and McMahon, 2009) also fully inhibited eIF4GI cleavage on infection of the cells with HRV8v.

Although the above assay measures arrival and translation of the viral RNA in the cytosol, we additionally addressed the effect of the drugs on entry via *de novo* viral protein synthesis. Cells grown on cover slips were pretreated with the drugs as in Fig. 9A but infected at 10 TCID$_{50}$/cell, a multiplicity of infection which only allows for detection of replicated virus; at this low MOI input virus remains below the detection limit of immunofluorescence microscopy. After incubation for 10 h at 34 °C, intracellular virus was stained as in Fig. 1 and the number of infected cells was determined with a TissueFAXS instrument. As seen in Fig. 9C, using production of viral protein as readout, except for cytochalasin, the inhibitor profile was quite similar to that derived from eIF4GI cleavage. The latter drug might only retard RNA arrival in the cytosol (as seen from the strong inhibition of the cleavage at 3 h pi) and replication could catch up during the longer incubation period used in the assay based on viral synthesis. However, this is so far purely hypothetic. Nevertheless, taken together, the data in Fig. 9 indicate that the drugs specifically affect entry and that the effects on viral replication are minor. Therefore, the results of these experiments strongly support the data derived from immunofluorescence microscopy colocalization and those of the dominant negative mutants of key proteins of the various entry pathways.

Dominant negative dynamin^{K44A} inhibits viral entry and replication

In order to support the finding of dynamin-dependent entry of HRV8v obtained with dynasore, we also carried out experiments by using the mutant dyn^{K44A}. This dominant negative inhibitor of dynamin 2 has been used in many studies to demonstrate dynamin dependence of endocytosis for a given ligand. A plasmid directing overexpression of wt dynamin (control) and mutant dynamin, respectively, was transfected into RD cells. After allowing for synthesis of the protein for 17 h, the cells were challenged with HRV8v at 20 TCID$_{50}$/cell and viral replication was monitored at 17 h pi by indirect immunofluorescence microscopy. These conditions were chosen as to obtain about 90% infected cells at the time of analysis. Fig. 10A demonstrates the absence of viral antigen in those cells actively producing dyn^{K44A} whereas virus production was not impaired in cells overexpressing the wt protein. About 95% of the cells overexpressing dyn^{wt} became infected, whereas in the dyn^{K44A} expressing cells only about 14% showed viral replication (Fig. 10B). This is in accordance with the inhibition of virus entry by dynasore (Fig. 9).

Electron microscopy of virus entry

The tubovesicular compartments involved in the diverse entry pathways exhibit characteristic morphological features and clathrin-coated pits, caveolae, and macropinocytic membrane invaginations are distinguishable by electron microscopy (EM). Apart from these, morphologically different tubular structures have been recently implicated in other uptake mechanisms (Lundmark et al., 2008). We thus studied entry of HRV8v by EM. RD cells were infected with HRV8v for the times indicated in Fig. 11 and thin sections were prepared. HRV8v was neither seen in coated pits/vesicles nor in tubular structures but was rather found in shallow invaginations of the plasma membrane. Many viruses aligned on the membrane and were taken up in large vesicular structures. At 20 min, they accumulated in irregularly shaped vesicles of about 0.5 μm diameter similar to those reported for macropinocytic uptake of adenovirus type 35 (Kalin et al., 2010). Importantly, as checked by EM of the inoculum, the viral preparation used for infection was not aggregated
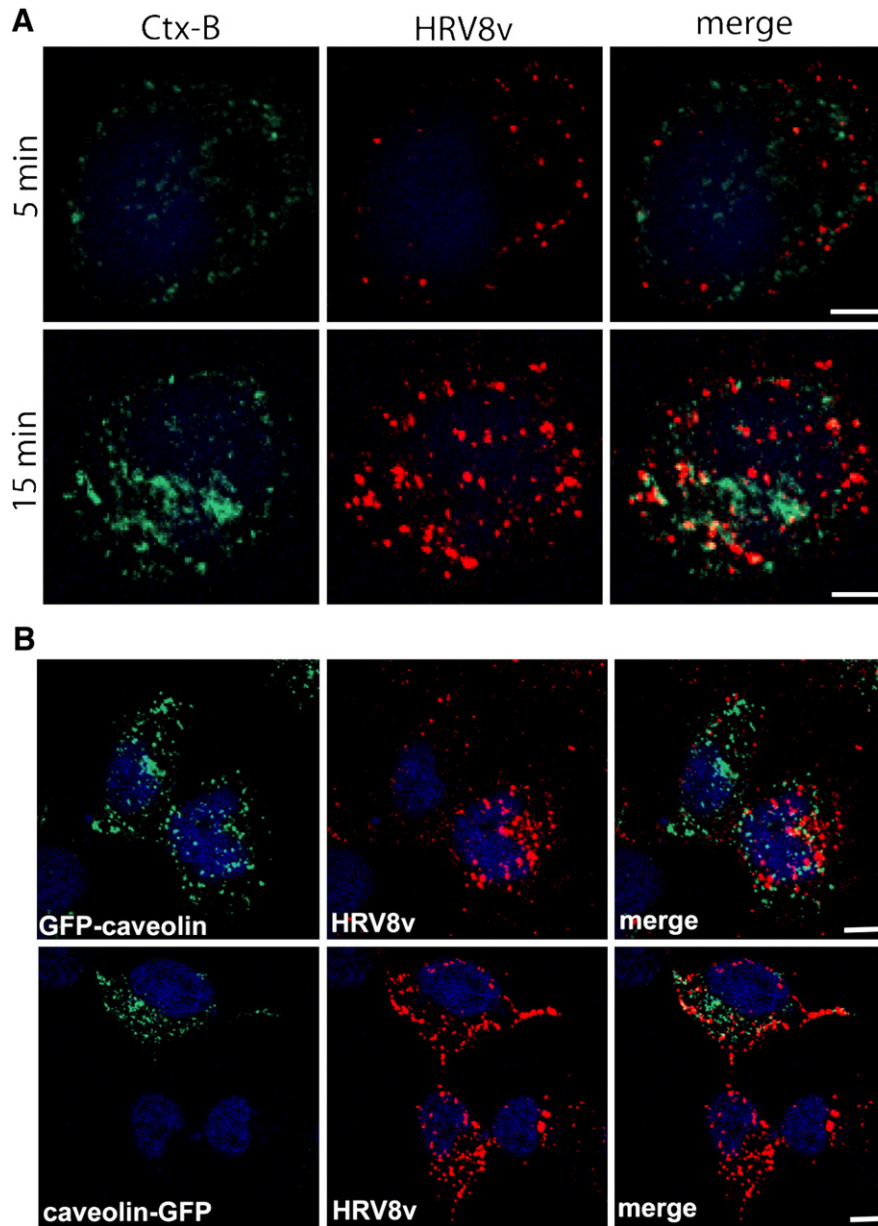
Fig. 6. HRV8v neither colocalizes with cholera toxin B nor with caveolin-1. A) RD cells were incubated with HRV8v at 500 $TCID_{50}$/cell in the presence of 1 μg/ml Alexa Fluor 488-CtxB for 5 and 15 min (continuous internalization) at 34 °C. Unbound material was washed away and cells were fixed and stained for virus with type-specific mouse antiserum followed by TxR-labeled secondary antibody. B) RD cells were transfected with pEGFP-caveolin-1 and caveolin-pEGFP, as indicated and after 24 h infected with HRV8v at 300 $TCID_{50}$/cell for 30 min at 34 °C. Cells were fixed and processed as above. Colocalization was assessed by confocal fluorescence microscopy as in Fig. 3. Bar, 10 μm.

(Fig. 11F). This suggests that the virions stick together only as soon as they contact the cells. The morphologic characteristics of the virus-filled vesicles are consistent with the previous results suggesting dynamin-dependent macropinocytosis as a plausible entry route for HRV8v bound to HS. It is of note that the ratio between infectious and non-infectious HRV particles is generally very low (Abraham and Colonno, 1984; Stott and Killington, 1972) and that we observed that HRV8v readily lost infectivity upon purification. Therefore, the concentration of physical viral particles is most likely much higher than the $TCID_{50}$/ml applied.

Discussion

Absence of co-localization with established markers of clathrin- and caveolin-dependent endocytosis demonstrated that HRV8v, when entering via HS, exploits neither of these pathways. Regarding the possible involvement of caveolin, in addition, we found much higher

expression of this protein in the ICAM-1 negative COS-7 cells than in RD cells. However, HRV8v entered the two cell lines with equal efficiency (data not shown). Thus, involvement of clathrin and caveolin is highly unlikely.

The pharmacological inhibitor profiles corroborated the immuno-fluorescence data. Taking cleavage of eIF4GI at 3 h pi as readout for successful entry, a possible influence of the drugs on later steps in infection, such as modification of RNA synthesis and/or virus release, as previously suggested for HRV2 (Gazina et al., 2005), was excluded. Of the compounds tested, amiloride and EIPA, inhibitors of Na^+/H^+ exchangers, and dynasore that blocks dynamin function, abolished cleavage of eIF4GI in RD cells challenged with HRV8v. The role of functional dynamin in HRV8v entry was also assessed by use of the dominant-negative dynamin mutant K44A whose overexpression strongly reduced viral replication. Cytochalasin D, an inhibitor of actin polymerization, inhibited cleavage strongly but not completely. A similar degree of inhibition of eIF4GI cleavage was seen with
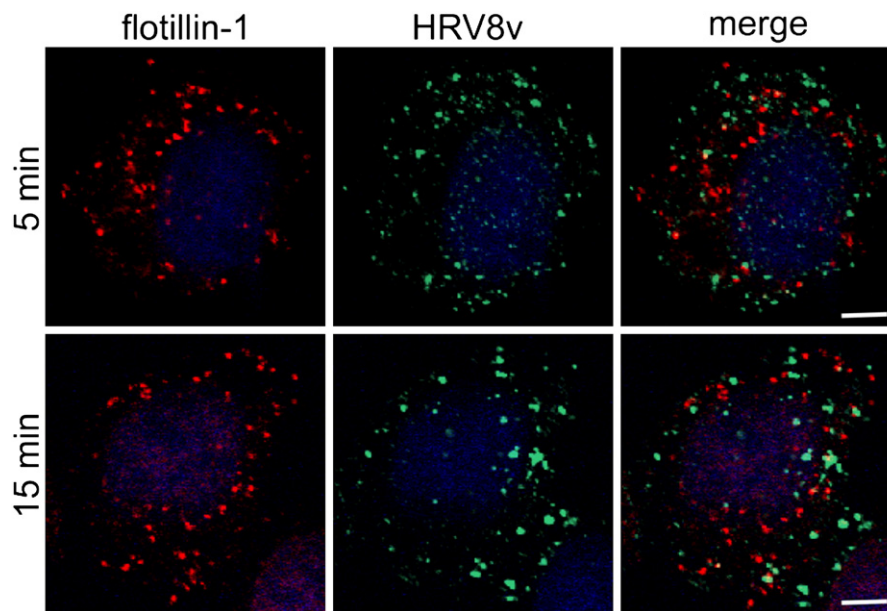
Fig. 7. Flotillin does not colocalize with HRV8v. RD cells were infected with HRV8v at 500 $TCID_{50}$/cell for 5 and 15 min at 37 °C (continuous internalization), unbound virus was removed, and the cells were fixed. Flotillin-1 was stained with rabbit anti-flotillin-1 antibody followed by TxR-conjugated secondary antibody. Virus was detected with type-specific antibody followed by Alexa Fluor 488-labeled secondary antibody. Cells were processed and viewed as in Fig. 3. One single confocal slice is shown. Bar, 10 μm.

wortmannin (not shown). However, since this drug had been found to also retard transfer of HRV2 from early to late endocytic compartments (Brabec et al., 2006), interpretation of this result is difficult.

We also measured viral uptake in the presence of drugs by automatically counting virus-replicating cells in a TissueFAXS instrument followed by quantification by the TissueQuest software. Except from the discrepancy with cytochalasin D, which showed weaker inhibition in these experiments when compared to the cleavage assay, the drug-inhibition profiles of the two methods are quite similar and again support the results of immunofluorescence microscopy. It is noteworthy that expression of the dominant negative mutants of amphiphysin and AP180 somewhat increased uptake of HRV8v. This is corroborated by a small increase in eIF4GI cleavage in the presence of chlorpromazine and nystatin, respectively. This might indicate that inhibition of CME and caveolin/lipid raft endocytosis results in an up-regulation of the pathway exploited by HRV8v. Collectively, the data strongly indicate a clathrin- and caveolin independent uptake of HRV8v via HS and rather point to one of the pathways discussed below.

Macropinocytosis and CLIC/GEEC (clathrin-independent carriers/GPI-enriched early endosomal compartments), are only recently becoming better defined via attempts at establishing a correlation of key proteins, such as flotillin, CtBP1/BARS (C-terminal binding protein 1/brefeldin A-ADP ribosylated substrate), and GRAF1 (GTPase regulator associated with focal adhesion kinase-1) with morphological characteristics (Hansen and Nichols, 2009; Lundmark et al., 2008). Experiments by Payne et al. (2007) on uptake of proteoglycan-binding ligands pointed to the involvement of flotillins. However, as flotillins require hetero-oligomerization for function (Babuke et al., 2009), lack of co-localization of HRV8v with flotillin-1 makes involvement of this and any other flotillin homologues highly unlikely. In macropinocytosis, at least in some cell types, vesicles are being severed from the plasma membrane by CtBP1/BARS (Bonazzi et al., 2005; Liberali et al., 2008), one of several homologues involved in transcriptional repression, Golgi to plasma membrane transport and endocytosis (Gallop et al., 2005). Since dynamin is definitely required for HRV8v entry, involvement of CtBP1/BARS is unlikely, as these two proteins exert similar but presumably mutually exclusive functions.

Amiloride and its more active derivative EIPA are generally accepted as relatively specific inhibitors of macropinocytosis. Like-

wise, drugs interfering with actin polymerization also inhibit macropinocytosis. Finally, stimulation of fluid phase uptake, usually determined via engulfment of fluorescent dextran, is widely accepted as an indicator for macropinocytosis. Cargo, such as dextran, thereby accumulates in comparatively large vesicles. Based on all these criteria, HRV8v enters via macropinocytosis. The weak (about 50%) inhibition by MßCD does not contradict this view as a role of cholesterol but not of caveolae in macropinocytosis has been demonstrated in A431 cells (Grimmer et al., 2002). On the other hand, in HRV8v endocytosis, dynamin apparently takes part in scission of the vesicles from the plasma membrane.

HRV14, when entering via ICAM-1, exhibits a very similar behavior with respect to co-localization with specific markers but its inhibitor profile is quantitatively different; inhibition by dynasore and cytochalasin D is only partial whereas there is virtually no inhibition by MßCD (Khan et al., 2010). However, it is possible that the 'natural' entry pathway is modified by the high expression level of ICAM-1 in the RD-ICAM cells (Khan et al., 2010). Unfortunately, the double specificity of HRV8v does not allow for assessing whether HRV14, bound to ICAM-1, and HRV8v, bound to HS, travel along the same pathway.

Most remarkably, HRV14 and HRV8v localized in morphologically different invaginations. HRV14 accumulated in long tubules in RD-ICAM cells (Khan et al., 2010) and in BHK cells overexpressing human ICAM-1 (Grunert et al., 1997) appearing similar to the tubular invaginations seen for adenovirus 3 entering HeLa cells by macropinocytosis (Amstutz et al., 2008). On the other hand, numerous, apparently aggregated HRV8v particles, were seen attached to the cellular surface. These localized, at 20 min pi, in relatively large (about 500 nm diameter) vesicles. The virions did not stick to each other prior to addition to the cells. Therefore, it is conceivable that HS shed from the cells (Fitzgerald et al., 2000; Fux et al., 2009) leads to this massive aggregation. We cannot exclude that this aggregation directs HRV8v into an unusual pathway not followed at much lower concentrations where the virions are presumably mono-disperse.

With respect to the strict requirement for dynamin, HRV8v differs from enterovirus 1 (EV1) entering in a clathrin and caveolin independent way via $\alpha_2\beta_1$ into Saos-2 human osteosarcoma cells transfected to express this integrin; in these cells, EV1 finally arrives in caveosomes (Karjalainen et al., 2008). It also differs from
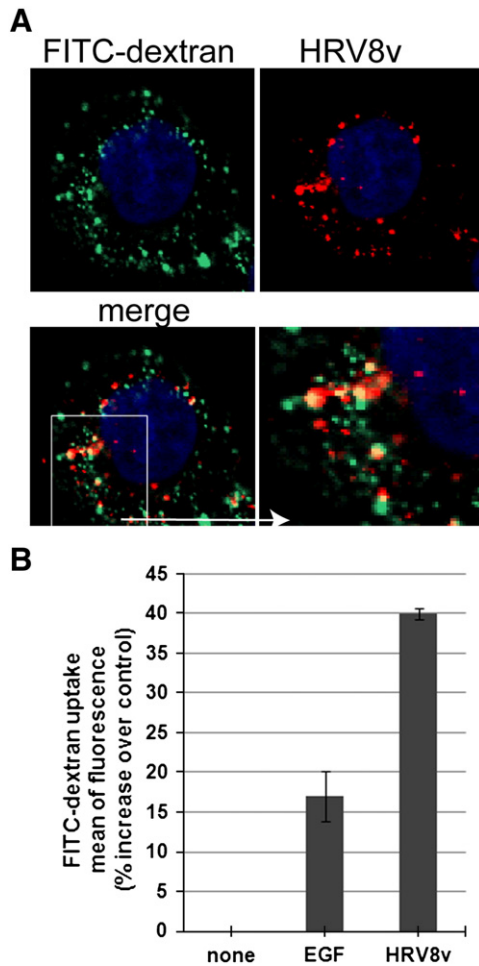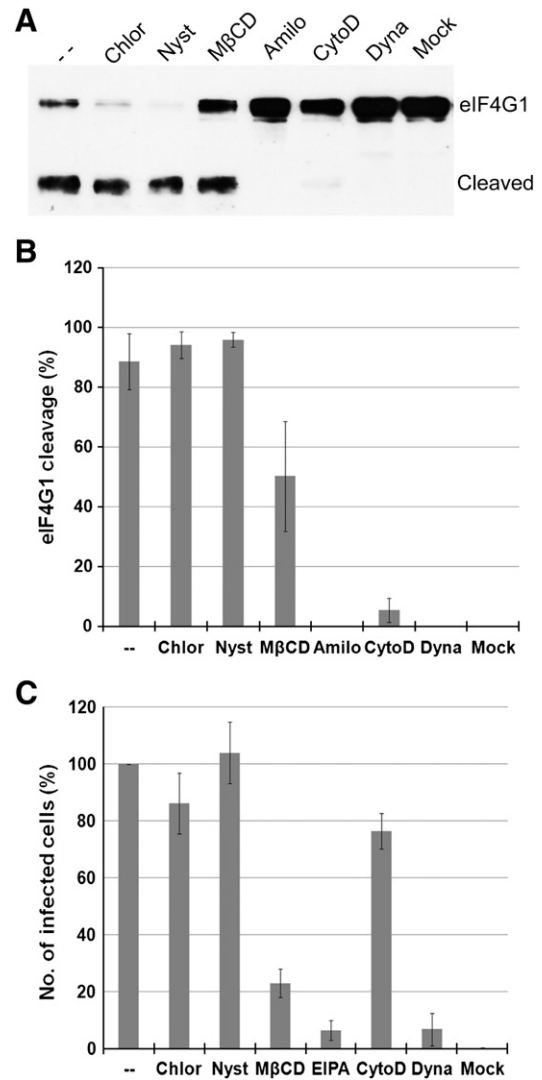
Fig. 8. HRV8v colocalizes with FITC-dextran and stimulates its uptake. A) RD cells were infected with HRV8v at 300 TCID$_{50}$/cell (continuous internalization) in the presence of 500 μg/ml lysine-fixable FITC-dextran at 34 °C for 15 min, washed, and prepared for immunofluorescence microscopy as in Fig. 3. Bar, 10 μm. B) FITC-dextran uptake was quantified by FACS analysis as the mean of cell-associated fluorescence at 10 min internalization. EGF was used as a control. The graph shows percent increase of the signal with respect to the mean fluorescence observed without stimulation (i.e. in the absence of EGF and HRV8v). Mean of 3 separate experiments ± SD.


Fig. 9. Inhibition profile of pharmacological inhibitors. Cells were grown in 24 well plates until 90% confluent. The drugs were added at the concentrations indicated in Materials and methods and incubated for 30 min. Then, virus was added at 300 TCID$_{50}$/cell and incubation continued for further 3 h. After removal of the supernatant, the cells were harvested in sample buffer and proteins were separated on a SDS 6% polyacrylamide gel. A) Cleavage of eIF4G1 was monitored via western blotting with a rabbit antiserum followed by HRP-conjugated anti-rabbit antibodies and proteins were detected by chemiluminescence recorded on X-ray film. B) Cleavage was quantified with ImageJ by using scanned films from three independent experiments, including the one shown in A). C) Infection was with 10 TCID$_{50}$/cell and viral entry plus replication was quantified at 10 h pi with a TissueFAXS instrument relating the cells infected in the presence of the drugs to the number of cells infected in the absence of inhibitors. Data are the mean of three independent experiments ± SD. Inhibitors used are indicated; –, control (no inhibitor); Chlor, chlorpromazine; Nyst, nystatin; MßCD, methyl-ß-cyclodextrin; Amilo, amiloride; CytoD, cytochalasin; Dyna, dynasore; Mock, mock-infected.

adenovirus 3 entering HeLa-ATCC cells via macropinocytosis upon binding to various α$_v$ integrins and CD46 (Amstutz et al., 2008), and from coxsackievirus B3 entry into Caco-2 cells by macropinocytosis exhibiting aspects of caveolar endocytosis (Coyne et al., 2007). Uptake of the former viruses does not require functional dynamin. However, at least in HeLa-K cells, adenovirus 3 and 35 appear to require dynamin (Amstutz et al., 2008; Kalin et al., 2010). Hence, our data provide additional evidence for the existence of a dynamin dependent but clathrin- and caveolin-independent uptake mechanism in RD cells. Very recently, Heikkila and colleagues similarly reported that Coxsackie A9 virus, when bound to integrin α$_v$ß$_6$, was taken up into A549 cells by some form of macropinocytosis dependent on dynamin in a clathrin and caveolin independent manner (Heikkila et al., 2010).

As demonstrated by inhibition with bafilomycin, HRV8v requires acidic pH for uncoating and productive infection when entering via HS. This is also supported by its co-localization with EEA1 at 37 °C at 30 min pi (data not shown). It thus differs from EV1, which travels from macropinosomes to (non-acidic) caveosomes, although not via caveolae (Karjalainen et al., 2008; Liberali et al., 2008). The viruses mentioned above use receptors different from HS but show various aspects of macropinocytosis. It is thus necessary to compare also

HRV8v uptake with that of another HS-binding picornavirus, the FMDV variant O$_1$C3056R. This virus enters MCF-10A cells via caveolae and is not inhibited by amiloride; it is not entirely clear whether it follows the classical caveolar pathway (O'Donnell et al., 2008). As FMDV also depends on low pH for infection, it must be directed into acidic compartments. Indeed, at least glycosylphosphatidylinositol (GPI)-anchored molecules entering via caveolae can reach endosomes (Maxfield and Mayor, 1997). Since most HS is linked to proteins carrying GPI (Filmus et al., 2008), viral arrival in acidic compartments is not unexpected. In any case, many distinct entry pathways converge in early (sorting) endosomes and consequently, in mildly acidic compartments (Jones, 2007). Vaccinia virus is yet another pathogen

A

B
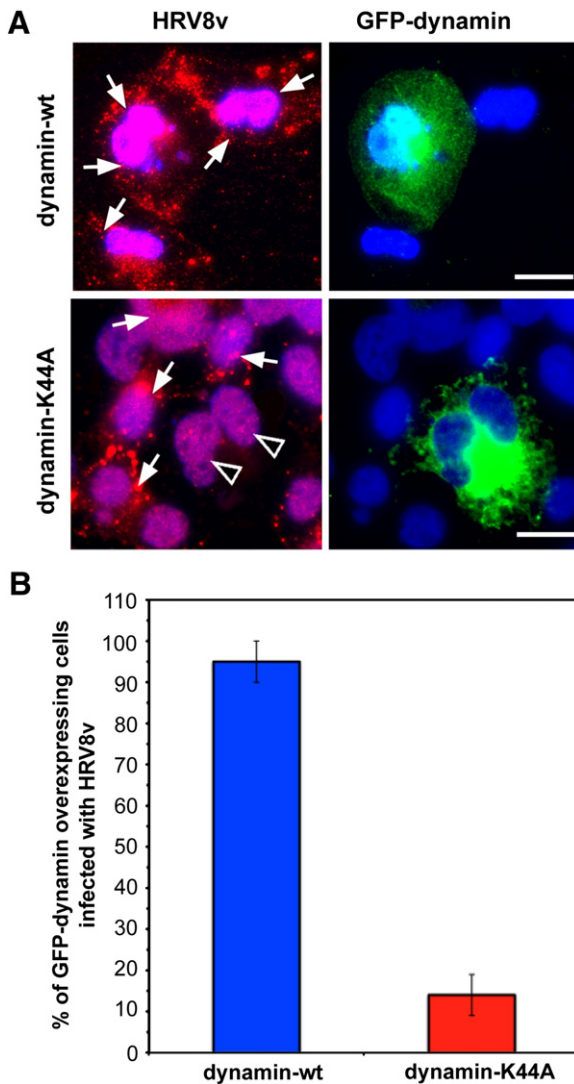
Fig. 10. Dominant negative inhibitor dyn[K44A] blocks HRV8v entry into RD cells. RD cells were transfected with a plasmid encoding GFP-tagged wt dynamin 2 and dominant negative mutant dyn[K44A], respectively and left for 17 h to allow for expression. Cells were challenged with HRV8v at 20 TCID$_{50}$/cell and fixed at 17 h pi. Virus was revealed with type specific antibody followed by Alexa586-labeled secondary antibody. A) Cells were processed and viewed under the fluorescence microscope. Bar, 10 μm. Arrows point to HRV8v-infected cells, arrowheads to uninfected cells. B) About 400 cells expressing GFP-dyn[wt] and GFP-dyn[K44A] were scored for viral replication, which is given as percentage. Data are the mean ± SEM of four experiments.

entering via HS; binding to HeLa cells leads to extensive blebbing, which might be required for uptake since blebbistatin resulted in a strong decrease in intracellular virus. Viral entry was prevented by EIPA but not by dynasore. However, the unusual apoptotic mimicry operating in this case adds a further dimension to this mechanism (Mercer and Helenius, 2008). Taken together, formation and final fate of vesicles possessing properties of macropinosomes depend on the cell type. The pathway exploited by HRV8v combines characteristics of 'classical' macropinocytosis with unusual features. So far, several virus types have been shown to exploit macropinocytosis-like uptake mechanisms to breach the cell membrane for infection (reviewed in Mercer and Helenius, 2009). Our work adds a major group subgenus A rhinovirus to this collection and demonstrates the existence of a dynamin-dependent macropinocytosis-like pathway in RD cells. It gradually becomes accepted that non-clathrin non-caveolin dependent pathways follow various mechanisms and strikingly differ in

different cell-types, a fact reflected in different drug-inhibition profiles and involvement of key proteins (Sandvig et al., 2008). To gain more insight into the contribution of receptor and virus to the mode of entry, where possible, the use of the same cell type will be mandatory in future studies of cellular uptake of different viruses.

Materials and methods

Cells and viruses

Rhabdomyosarcoma (RD) cells, wt and stably transfected with human ICAM-1 (RD-ICAM), a kind gift of Darren Shafren (Univ. of Newcastle, Australia), were cultured as previously described (Khan et al., 2010; Newcombe et al., 2003). HeLa-H1 cells (for short called HeLa cells) were grown in MEM supplemented with 10% heat inactivated fetal calf serum (FCS), 100 U/ml penicillin, 100 μg/ml streptomycin, and 2 mM L-glutamine. For infection, DMEM supplemented with 30 mM MgCl$_2$, 2% FCS, and antibiotics (infection medium) was used. CHO-K1 cells and CHO mutants (pgsA-745 and pgsD-677) deficient in proteoglycan biosynthesis and HRVs were originally obtained from the ATCC; HRV8v, a variant of HRV8 replicating in RD cells was obtained by 3 serial passages alternating between HeLa and RD cells as previously described for HRV89 (Reischl et al., 2001). Briefly, RD cells were challenged with HRV8 at 100 TCID$_{50}$/cell in 24 well plates. After a 48 h incubation at 34 °C, the cells were broken and cleared supernatants were transferred onto HeLa cells. After 24 h, the HeLa cells were broken and the supernatants were transferred to RD cells. This procedure was repeated twice. Serotypic identity of variant and wt was confirmed by neutralization with type-specific guinea pig antiserum against HRV8 from ATCC. All experiments were conducted with three-time plaque-purified virus.

Virus binding and infection assays

HRV8 was labeled using standard methods. Cells grown in 24 well plates up to 90% confluency were challenged with [^{35}S]-labeled HRV8 at 12,000 cpm for 1 h at room temperature. Cells were washed with ice cold PBS, trypsinized and collected in scintillation vials. Cell-associated radioactivity was measured by liquid scintillation counting. For binding inhibition assays, RD cells were challenged with radioactive virus as above in the presence or absence of 2 mg/ml heparin for 1 h and processed for scintillation counting as above. For infection of RD cells and its inhibition with heparin, cells were grown in 96 well plates up to 70% confluency and infected with HRV8v at 10 TCID$_{50}$/cell in the presence or absence of 2 mg/ml heparin. After 24 h incubation at 34 °C, cell death was assessed by staining the cells with crystal violet.

Acid sensitivity of the virus

Virus at about 10^7 TCID$_{50}$ was incubated with isotonic 100 mM MES buffer of the pH values given in Fig. 1 for 30 min at 34 °C and neutralized with 0.5 M Na$_3$PO$_4$. Infectivity was determined by an end point dilution assay (Khan et al., 2007).

Antibodies and reagents

Mouse anti-HRV8, rabbit anti-HRV89, and rabbit anti-HRV14 were produced following standard protocols. For co-localization experiments, combinations of antibodies from different species were used. Rabbit anti-caveolin and rabbit anti-flotillin-1 antibodies were purchased from Santa Cruz Biotechnology. Secondary antibodies labeled with Texas red, Alexa Fluor 488, and Alexa Fluor 591, respectively, were from Jackson ImmunoResearch Laboratories and Molecular Probes, Invitrogen, respectively. Alexa Fluor 568 transferrin, Alexa Fluor 488 cholera toxin-B, and lysine-fixable FITC-dextran
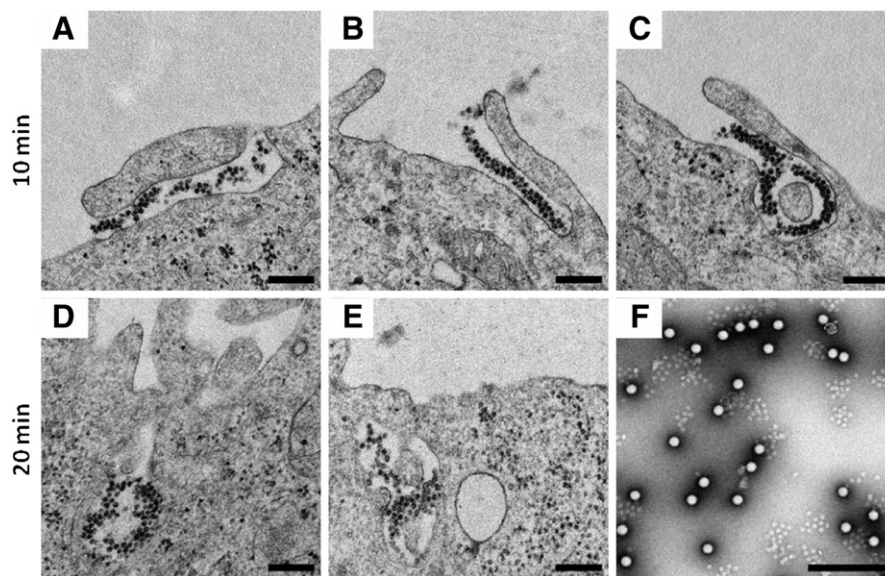
Fig. 11. Transmission electron microscopy of thin sections of cells infected with HRV8v. RD cells grown on cover slips were infected with HRV8v at 170 TCID$_{50}$/cell for the times indicated at 34 °C. Cells were treated with glutaraldehyde and OsO$_4$, embedded in resin, cut into 70 nm slices, and viewed at 36,000× magnification. Several fields are shown for better appreciation. The lower right panel shows HRV8v (at 56,000×) suspended in serum-free infection medium as it was used for inoculation. It indicates lack of aggregation in the absence of cells. Bar, 200 nm.

were from Molecular Probes, Invitrogen. The following drugs were purchased from Sigma, stock solutions made in the indicated solvents and used at the final concentrations given in parentheses; chlorpromazine in PBS (5 μg/ml); nystatin in DMSO (10 μg/ml); MßCD in PBS (5 mM), amiloride (5 mM), cytochalasin D (10 μg/ml), dynasore (80 μM), and EIPA (40 μM) all in DMSO.

Drug treatment

RD cells were seeded in 24 well plates, pre-incubated in the presence or absence of the respective drug for 30 min and infected with HRV8v at 300 TCID$_{50}$/cell. Samples were harvested in 50 μl sample buffer at 3 h pi for assessment of eIF4GI cleavage via western blotting. Drugs were present throughout the incubation. To evaluate entry plus replication, cells grown on coverslips were preincubated with the drugs as above but with slightly lower concentrations to avoid cytotoxicity due to the longer incubation period; chlorpromazine, MßCD, and cytochalasin D were used at 3 μg/ml, 3 mM and 5 μg/ml respectively. Amiloride was replaced with EIPA, which was used at 40 μM. Cells were challenged with virus at 10 TCID$_{50}$/cell and further incubated. At 10 h pi, they were washed, fixed, and stained for *de novo* synthesized viral protein as described below. The percentage of infected cells was determined with a TissueFAXS, quantified with TissueQuest software (TissueGnostics) and related to those infected in the absence of drugs. The mask (i.e. the kind of staining to be considered by the program as infection) was manually adjusted by comparing infected cells and cells in which uncoating (and infection) was prevented by bafilomycin. This also served as control for 'background' immunostaining of input virus. In each experiment, 10,000 cells were counted.

Western blot analysis

Proteins from whole cell lysates from each drug treatment were separated on a SDS-6% polyacrylamide gel and electro-transferred onto a PVDF membrane. The membrane was blocked with 5% milk powder in PBS containing 0.1% Triton X100 (PBS/T), incubated with rabbit anti-eIF4GI (1:8000) kindly donated by R. Rhoads, Louisiana

State University, USA, followed by HRP-labeled anti-rabbit antibody (1:20,000; Jackson Laboratories). Uncleaved and cleaved eIF4GI were visualized on X-ray film by using the ECL chemiluminescence detection system (Thermoscientific). Proteolysis was quantified from the scanned films with ImageJ (http://rsbweb.nih.gov/ij/).

Confocal fluorescence microscopy

Cells were grown on glass cover slips until 40–50% confluent. After washing with serum-free medium, they were challenged with virus at TCID$_{50}$/cell as specified in the figure legends. Unbound virus was removed by three washings with PBS^{++} (PBS with 1 mM MgCl$_2$ and 1 mM CaCl$_2$). Cells were fixed with 4% paraformaldehyde, and permeabilized in 0.2% Triton X100 for 5 min. After quenching with 50 mM NH$_4$Cl for 10 min, unspecific binding sites were blocked with 1% goat serum for either 1 h at room temperature or overnight at 4 °C. Cells were further incubated for 1 h at room temperature with primary antibody (1:500), washed 3 times with PBS^{++}, followed by secondary antibody (1:400), all diluted in 1% goat serum. Nuclei were stained with 0.1 μg/ml DAPI. For assessment of colocalization, cells were infected in the presence of 10 μg/ml Alexa Fluor 568 transferrin, 1 μg/ml Alexa Fluor 488 CtxB, and 500 μg/ml lysine-fixable fluorescein-dextran (70 kDa), respectively. Unbound material was removed and cells were fixed. Virus was detected by using type-specific antibodies as above. Cover slips were mounted in Moviol and viewed in a LSM510 Meta Carl Zeiss confocal microscope. Stacks were spaced by 0.5 μm. Contrast of the pictures was adjusted with LSM Image Browser (Carl Zeiss); lettering was done in Adobe Photoshop. Colocalization was quantified by using BioImageXD software (http://www.bioimagexd.net).

Transfection

The plasmids pEGFP-C3, encoding the clathrin light chain fused to green fluorescent protein (GFP-clathrin), myc-tagged pCMV-Amph-SH3, and pMCV-AP180 were kind gifts from Luc Snyers, Med. Univ. Vienna. They have been used and described previously (Snyers et al., 2003).

Plasmids pEGFP-caveolin, caveolin-pEGFP, and pEGFP-N1 (Dynamin-2 wild type and the mutant K44A) were kindly provided by Ari Helenius, Zurich, Switzerland. Cells were seeded on cover slips in 24 well plates and grown to 30% confluency. One μg plasmid DNA was mixed with 50 μl Optimem (Gibco). Separately, 2 to 3 μl Lipofectamine 2000 (Invitrogen) was mixed with 50 μl Optimem and incubated for 5 min at room temperature; the 2 solutions were mixed gently and incubation continued for 20 min. Cells were washed twice with antibiotic-free growth medium and laid down with 500 μl of the same medium. The mixture of plasmid DNA and Lipofectamine 2000 was applied onto the cells drop by drop with gentle rotation to avoid cell toxicity. Cells were incubated for 3 h with the mixture; the medium was then replaced with fresh antibiotic-free growth medium. Twenty-four hours post transfection cells were infected with the respective virus and processed for immunofluorescence microscopy. For Amphi-SH3 and AP-180C anti-myc antibody was used to detect expression. In case of the dynamin-2 constructs, after 17 h, cells were infected at 20 $TCID_{50}$/cell and stained for virus synthesis at 17 h pi.

Uptake of FITC-dextran

RD cells were grown in 24 well plates up to 90% confluence and incubated with serum-free medium for 4 h at 37 °C. Lysine-fixable FITC-dextran at 0.5 mg/ml was added in the presence or absence of HRV8v at 1000 $TCID_{50}$/cell and 100 ng/ml EGF, respectively, and incubated for the times indicated in the figure legends. Cells were washed with ice cold PBS and detached with trypsin at 4 °C, collected and resuspended in PBS containing 7% FCS. In each experiment, the mean fluorescence of 10,000 cells was determined in a BD FACS Calibur.

Electron microscopy

RD cells were seeded on Aclar cover-slips in 24 well plates and grown to almost 100% confluency. Cells were washed and infected with HRV8v at 170 $TCID_{50}$/cell. Note, however, that due to the well known high ratio between physical particles and infectious units the virus concentration might be more than 1000 times higher (Stott and Killington, 1972). After incubation at 34 °C for the given times, cells were washed twice with PBS and fixed with 2% freshly prepared glutaraldehyde for 1 h at room temperature. Cells were washed three times with 0.1 M Sorensen buffer (pH 7.3) and incubated for 1 h in 2% osmium tetroxide in the same buffer. After washing, cells were dehydrated in ascending concentrations of ethanol (40%–60%–80%–95% and 100%; kept over a molecular sieve), incubated with Epon/100% EtOH (1:1) and twice with Epon only, for 30 min each, embedded in resin-filled beam capsule lids, and incubated at 60 °C to polymerize for 2 days. Sections of 70 nm were prepared, stained with 2% uranyl acetate and lead citrate for 10 and 5 min respectively. Purified virus, taken up in serum-free infection medium was adsorbed to glow-discharged carbon-coated copper grids for 1 min, washed and stained with 2% Na-phosphotungstate (pH 7.4) for 1 min. Samples were viewed under an FEI Morgagni 80 kV electron microscope equipped with an 11 megapixel CCD camera.

Supplementary materials related to this article can be found online at doi:10.1016/j.virol.2010.12.042.

Acknowledgments

References

Abraham, G., Colonno, R.J., 1984. Many rhinovirus serotypes share the same cellular receptor. J. Virol. 51, 340–345.

Akula, S.M., Naranatt, P.P., Walia, N.S., Wang, F.Z., Fegley, B., Chandran, B., 2003. Kaposi's sarcoma-associated herpesvirus (human herpesvirus 8) infection of human fibroblast cells occurs through endocytosis. J. Virol. 77, 7978–7990.

Amstutz, B., Gastaldelli, M., Kalin, S., Imelli, N., Boucke, K., Wandeler, E., Mercer, J., Hemmi, S., Greber, U.F., 2008. Subversion of CtBP1-controlled macropinocytosis by human adenovirus serotype 3. EMBO J. 27, 956–969.

Babuke, T., Ruonala, M., Meister, M., Amaddii, M., Genzler, C., Esposito, A., Tikkanen, R., 2009. Hetero-oligomerization of reggie-1/flotillin-2 and reggie-2/flotillin-1 is required for their endocytosis. Cell. Signal. 21, 1287–1297.

Baravalle, G., Schober, D., Huber, M., Bayer, N., Murphy, R.F., Fuchs, R., 2005. Transferrin recycling and dextran transport to lysosomes is differentially affected by bafilomycin, nocodazole, and low temperature. Cell Tissue Res. 320, 99–113.

Bayer, N., Schober, D., Prchla, E., Murphy, R.F., Blaas, D., Fuchs, R., 1998. Effect of bafilomycin A1 and nocodazole on endocytic transport in HeLa cells: implications for viral uncoating and infection. J. Virol. 72, 9645–9655.

Bayer, N., Prchla, E., Schwab, M., Blaas, D., Fuchs, R., 1999. Human rhinovirus HRV14 uncoats from early endosomes in the presence of bafilomycin. FEBS Lett. 463, 175–178.

Bayer, N., Schober, D., Huttinger, M., Blaas, D., Fuchs, R., 2001. Inhibition of clathrin-dependent endocytosis has multiple effects on human rhinovirus serotype 2 cell entry. J. Biol. Chem. 276, 3952–3962.

Bishop, J.R., Schuksz, M., Esko, J.D., 2007. Heparan sulphate proteoglycans fine-tune mammalian physiology. Nature 446, 1030–1037.

Bonazzi, M., Spano, S., Turacchio, G., Cericola, C., Valente, C., Colanzi, A., Kweon, H.S., Hsu, V.W., Polishchuck, E.V., Polishchuck, R.S., Sallese, M., Pulvirenti, T., Corda, D., Luini, A., 2005. CtBP3/BARS drives membrane fission in dynamin-independent transport pathways. Nat. Cell Biol. 7, 570–580.

Brabec, M., Baravalle, G., Blaas, D., Fuchs, R., 2003. Conformational changes, plasma membrane penetration, and infection by human rhinovirus type 2: role of receptors and low pH. J. Virol. 77, 5370–5377.

Brabec, M., Blaas, D., Fuchs, R., 2006. Wortmannin delays transfer of human rhinovirus serotype 2 to late endocytic compartments. Biochem. Biophys. Res. Commun. 348, 741–749.

Coyne, C.B., Shen, L., Turner, J.R., Bergelson, J.M., 2007. Coxsackievirus entry across epithelial tight junctions requires occludin and the small GTPases Rab34 and Rab5. Cell Host Microbe 2, 181–192.

Doherty, G.J., McMahon, H.T., 2009. Mechanisms of endocytosis. Annu. Rev. Biochem. 78, 857–902.

Duchardt, F., Fotin-Mleczek, M., Schwarz, H., Fischer, R., Brock, R., 2007. A comprehensive model for the cellular uptake of cationic cell-penetrating peptides. Traffic 8, 848–866.

Falcone, S., Cocucci, E., Podini, P., Kirchhausen, T., Clementi, E., Meldolesi, J., 2006. Macropinocytosis: regulated coordination of endocytic and exocytic membrane traffic events. J. Cell Sci. 119, 4758–4769.

Fan, T.C., Chang, H.T., Chen, I.W., Wang, H.Y., Chang, M.D., 2007. A heparan sulfate-facilitated and raft-dependent macropinocytosis of eosinophil cationic protein. Traffic 8, 1778–1795.

Filmus, J., Capurro, M., Rast, J., 2008. Glypicans. Genome Biol. 9, 224.221–224.226.

Fitzgerald, M.L., Wang, Z., Park, P.W., Murphy, G., Bernfield, M., 2000. Shedding of syndecan-1 and -4 ectodomains is regulated by multiple signaling pathways and mediated by a TIMP-3-sensitive metalloproteinase. J. Cell Biol. 148, 811–824.

Ford, M.G., Pearse, B.M., Higgins, M.K., Vallis, Y., Owen, D.J., Gibson, A., Hopkins, C.R., Evans, P.R., McMahon, H.T., 2001. Simultaneous binding of PtdIns(4,5)P2 and clathrin by AP180 in the nucleation of clathrin lattices on membranes. Science 291, 1051–1055.

Fux, L., Ilan, N., Sanderson, R.D., Vlodavsky, I., 2009. Heparanase: busy at the cell surface. Trends Biochem. Sci. 34, 511–519.

Gallop, J.L., Butler, P.J., McMahon, H.T., 2005. Endophilin and CtBP/BARS are not acyl transferases in endocytosis or Golgi fission. Nature 438, 675–678.

Gazina, E.V., Harrison, D.N., Jefferies, M., Tan, H., Williams, D., Anderson, D.A., Petrou, S., 2005. Ion transport blockers inhibit human rhinovirus 2 release. Antivir. Res. 67, 98–106.

Glebov, O.O., Bright, N.A., Nichols, B.J., 2006. Flotillin-1 defines a clathrin-independent endocytic pathway in mammalian cells. Nat. Cell Biol. 8, 46–54.

Gradi, A., Svitkin, Y.V., Imataka, H., Sonenberg, N., 1998. Proteolysis of human eukaryotic translation initiation factor eIF4GII, but not eIF4GI, coincides with the shutoff of host protein synthesis after poliovirus infection. Proc. Natl. Acad. Sci. U. S. A. 95, 11089–11094.

Greve, J.M., Forte, C.P., Marlor, C.W., Meyer, A.M., Hoverlitty, H., Wunderlich, D., McClelland, A., 1991. Mechanisms of receptor-mediated rhinovirus neutralization defined by two soluble forms of ICAM-1. J. Virol. 65, 6015–6023.

Grimmer, S., van Deurs, B., Sandvig, K., 2002. Membrane ruffling and macropinocytosis in A431 cells require cholesterol. J. Cell Sci. 115, 2953–2962.

Gruenberger, M., Pevear, D., Diana, G.D., Kuechler, E., Blaas, D., 1991. Stabilization of human rhinovirus serotype-2 against pH-induced conformational change by antiviral compounds. J. Gen. Virol. 72, 431–433.

Grunert, H.P., Wolf, K.U., Langner, K.D., Sawitzky, D., Habermehl, K.O., Zeichhardt, H., 1997. Internalization of human rhinovirus 14 into HeLa and ICAM-1-transfected BHK cells. Med. Microbiol. Immunol. 186, 1–9.

Hansen, C.G., Nichols, B.J., 2009. Molecular mechanisms of clathrin-independent endocytosis. J. Cell Sci. 122, 1713–1721.

Hansen, G.H., Dalskov, S.M., Rasmussen, C.R., Immerdal, L., Niels-Christiansen, L.L., Danielsen, E.M., 2005. Cholera toxin entry into pig enterocytes occurs via a lipid raft- and clathrin-dependent mechanism. Biochemistry 44, 873–882.

Heikkila, O., Susi, P., Tevaluoto, T., Harma, H., Marjomaki, V., Hyypia, T., Kiljunen, S., 2010. Internalization of coxsackievirus A9 is mediated by {beta}2-microglobulin, dynamin, and Arf6 but not by caveolin-1 or clathrin. J. Virol. 84, 3666–3681.

Heikkinen, T., Jarvinen, A., 2003. The common cold. Lancet 361, 51–59.

Hofer, F., Gruenberger, M., Kowalski, H., Machat, H., Huettinger, M., Kuechler, E., Blaas, D., 1994. Members of the low density lipoprotein receptor family mediate cell entry of a minor-group common cold virus. Proc. Natl. Acad. Sci. U. S. A. 91, 1839–1842.

Irurzun, A., Carrasco, L., 2001. Entry of poliovirus into cells is blocked by valinomycin and concanamycin A. Biochemistry 40, 3589–3600.

Jones, A.T., 2007. Macropinocytosis: searching for an endocytic identity and role in the uptake of cell penetrating peptides. J. Cell. Mol. Med. 11, 670–684.

Kalin, S., Amstutz, B., Gastaldelli, M., Wolfrum, N., Boucke, K., Havenga, M., Digennaro, F., Liska, N., Hemmi, S., Greber, U.F., 2010. Macropinocytotic uptake and infection of human epithelial cells with species B2 adenovirus type 35. J. Virol. 84, 5336–5350.

Karjalainen, M., Kakkonen, E., Upla, P., Paloranta, H., Kankaanpaa, P., Liberali, P., Renkema, G.H., Hyypia, T., Heino, J., Marjomaki, V., 2008. A Raft-derived, Pak1-regulated entry participates in alpha2beta1 integrin-dependent sorting to caveosomes. Mol. Biol. Cell 19, 2857–2869.

Khan, A.G., Pichler, J., Rosemann, A., Blaas, D., 2007. Human rhinovirus type 54 infection via heparan sulfate is less efficient and strictly dependent on low endosomal pH. J. Virol. 81, 4625–4632.

Khan, A.G., Pickl-Herk, A., Gajdzik, L., Marlovits, T., Fuchs, R., Blaas, D., 2010. Human rhinovirus 14 enters rhabdomyosarcoma cells expressing ICAM-1 by a clathrin, caveolin, and flotillin-independent pathway. J. Virol. 84, 3984–3992.

Koivusalo, M., Welch, C., Hayashi, H., Scott, C.C., Kim, M., Alexander, T., Touret, N., Hahn, K.M., Grinstein, S., 2010. Amiloride inhibits macropinocytosis by lowering submembranous pH and preventing Rac1 and Cdc42 signaling. J. Cell Biol. 188, 547–563.

Konecsni, T., Berka, U., Pickl-Herk, A., Bilek, G., Khan, A.G., Gajdzig, L., Fuchs, R., Blaas, D., 2009. Low pH-triggered beta-propeller switch of the low-density lipoprotein receptor assists rhinovirus infection. J. Virol. 83, 10922–10930.

Liberali, P., Kakkonen, E., Turacchio, G., Valente, C., Spaar, A., Perinetti, G., Bockmann, R.A., Corda, D., Colanzi, A., Marjomaki, V., Luini, A., 2008. The closure of Pak1-dependent macropinosomes requires the phosphorylation of CtBP1/BARS. EMBO J. 27, 970–981.

Lundmark, R., Doherty, G.J., Howes, M.T., Cortese, K., Vallis, Y., Parton, R.G., McMahon, H.T., 2008. The GTPase-activating protein GRAF1 regulates the CLIC/GEEC endocytic pathway. Curr. Biol. 18, 1802–1808.

Macia, E., Ehrlich, M., Massol, R., Boucrot, E., Brunner, C., Kirchhausen, T., 2006. Dynasore, a cell-permeable inhibitor of dynamin. Dev. Cell 10, 839–850.

Marlovits, T.C., Abrahamsberg, C., Blaas, D., 1998. Very-low-density lipoprotein receptor fragment shed from HeLa cells inhibits human rhinovirus infection. J. Virol. 72, 10246–10250.

Masereel, B., Pochet, L., Laeckmann, D., 2003. An overview of inhibitors of Na(+)/H(+) exchanger. Eur. J. Med. Chem. 38, 547–554.

Maxfield, F.R., Mayor, S., 1997. Cell surface dynamics of GPI-anchored proteins. Adv. Exp. Med. Biol. 419, 355–364.

McErlean, P., Shackelton, L.A., Andrews, E., Webster, D.R., Lambert, S.B., Nissen, M.D., Sloots, T.P., Mackay, I.M., 2008. Distinguishing molecular features and clinical characteristics of a putative new rhinovirus species, human rhinovirus C (HRV C). PLoS ONE 3, e1847.

Meier, O., Boucke, K., Hammer, S.V., Keller, S., Stidwill, R.P., Hemmi, S., Greber, U.F., 2002. Adenovirus triggers macropinocytosis and endosomal leakage together with its clathrin-mediated uptake. J. Cell Biol. 158, 1119–1131.

Mercer, J., Helenius, A., 2008. Vaccinia virus uses macropinocytosis and apoptotic mimicry to enter host cells. Science 320, 531–535.

Mercer, J., Helenius, A., 2009. Virus entry by macropinocytosis. Nat. Cell Biol. 11, 510–520.

Neubauer, C., Frasel, L., Kuechler, E., Blaas, D., 1987. Mechanism of entry of human rhinovirus 2 into HeLa cells. Virology 158, 255–258.

Newcombe, N.G., Andersson, P., Johansson, E.S., Au, G.G., Lindberg, A.M., Barry, R.D., Shafren, D.R., 2003. Cellular receptor interactions of C-cluster human group A coxsackieviruses. J. Gen. Virol. 84, 3041–3050.

Nurani, G., Lindqvist, B., Casasnovas, J.M., 2003. Receptor priming of major group human rhinoviruses for uncoating and entry at mild low-pH environments. J. Virol. 77, 11985–11991.

O'Donnell, V., Larocco, M., Baxt, B., 2008. Heparan sulfate-binding foot-and-mouth disease virus enters cells via caveola-mediated endocytosis. J. Virol. 82, 9075–9085.

Palmenberg, A.C., Spiro, D., Kuzmickas, R., Wang, S., Djikeng, A., Rathe, J.A., Fraser-Liggett, C.M., Liggett, S.B., 2009. Sequencing and analyses of all known human rhinovirus genomes reveal structure and evolution. Science 324, 55–59.

Payne, C.K., Jones, S.A., Chen, C., Zhuang, X., 2007. Internalization and trafficking of cell surface proteoglycans and proteoglycan-binding ligands. Traffic 8, 389–401.

Pelkmans, L., Kartenbeck, J., Helenius, A., 2001. Caveolar endocytosis of simian virus 40 reveals a new two-step vesicular-transport pathway to the ER. Nat. Cell Biol. 3, 473–483.

Poon, G.M., Gariepy, J., 2007. Cell-surface proteoglycans as molecular portals for cationic peptide and polymer entry into cells. Biochem. Soc. Trans. 35, 788–793.

Prchla, E., Kuechler, E., Blaas, D., Fuchs, R., 1994. Uncoating of human rhinovirus serotype 2 from late endosomes. J. Virol. 68, 3713–3723.

Pu, Y., Zhang, X., 2008. Mouse hepatitis virus type 2 enters cells through a clathrin-mediated endocytic pathway independent of Eps15. J. Virol. 82, 8112–8123.

Raghu, H., Sharma-Walia, N., Veettil, M.V., Sadagopan, S., Chandran, B., 2009. Kaposi's sarcoma-associated herpesvirus utilizes an actin polymerization-dependent macropinocytic pathway to enter human dermal microvascular endothelial and human umbilical vein endothelial cells. J. Virol. 83, 4895–4911.

Reischl, A., Reithmayer, M., Winsauer, G., Moser, R., Gosler, I., Blaas, D., 2001. Viral evolution toward change in receptor usage: adaptation of a major group human rhinovirus to grow in ICAM-1-negative cells. J. Virol. 75, 9312–9319.

Sandvig, K., Torgersen, M.L., Raa, H.A., van Deurs, B., 2008. Clathrin-independent endocytosis: from nonexisting to an extreme degree of complexity. Histochem. Cell Biol. 129, 267–276.

Schneider, B., Schueller, C., Utermoehlen, O., Haas, A., 2007. Lipid microdomain-dependent macropinocytosis determines compartmentation of *Afipia felis*. Traffic 8, 226–240.

Schnitzer, J.E., Oh, P., Pinney, E., Allard, J., 1994. Filipin-sensitive caveolae-mediated transport in endothelium: reduced transcytosis, scavenger endocytosis, and capillary permeability of select macromolecules. J. Cell Biol. 127, 1217–1232.

Smart, E.J., Anderson, R.G., 2002. Alterations in membrane cholesterol that affect structure and function of caveolae. Methods Enzymol. 353, 131–139.

Snyers, L., Zwickl, H., Blaas, D., 2003. Human rhinovirus type 2 is internalized by clathrin-mediated endocytosis. J. Virol. 77, 5360–5369.

Spillmann, D., 2001. Heparan sulfate: anchor for viral intruders? Biochimie 83, 811–817.

Stott, E.J., Killington, R.A., 1972. Rhinoviruses. Annu. Rev. Microbiol. 26, 503–524.

Stuart, A.D., Eustace, H.E., McKee, T.A., Brown, T.D., 2002. A novel cell entry pathway for a DAF-using human enterovirus is dependent on lipid rafts. J. Virol. 76, 9307–9322.

Torgersen, M.L., Skretting, G., van Deurs, B., Sandvig, K., 2001. Internalization of cholera toxin by different endocytic mechanisms. J. Cell Sci. 114, 3737–3747.

Uncapher, C.R., Dewitt, C.M., Colonno, R.J., 1991. The major and minor group receptor families contain all but one human rhinovirus serotype. Virology 180, 814–817.

Van Hamme, E., Dewerchin, H.L., Cornelissen, E., Verhasselt, B., Nauwynck, H.J., 2008. Clathrin- and caveolae-independent entry of feline infectious peritonitis virus in monocytes depends on dynamin. J. Gen. Virol. 89, 2147–2156.

Vlasak, M., Goesler, I., Blaas, D., 2005a. Human rhinovirus type 89 variants use heparan sulfate proteoglycan for cell attachment. J. Virol. 79, 5963–5970.

Vlasak, M., Roivainen, M., Reithmayer, M., Goesler, I., Laine, P., Snyers, L., Hovi, T., Blaas, D., 2005b. The minor receptor group of human rhinovirus (HRV) includes HRV23 and HRV25, but the presence of a lysine in the VP1 HI loop is not sufficient for receptor binding. J. Virol. 79, 7389–7395.

West, M.A., Bretscher, M.S., Watts, C., 1989. Distinct endocytotic pathways in epidermal growth factor-stimulated human carcinoma A431 cells. J. Cell Biol. 109, 2731–2739.

Wigge, P., Vallis, Y., McMahon, H.T., 1997. Inhibition of receptor-mediated endocytosis by the amphiphysin SH3 domain. Curr. Biol. 7, 554–560.